What's underneath?

Non-destructive depth profile of painted stratigraphies by synchrotron grazing incidence X-ray diffraction

Elena Possenti,[a, b *] Chiara Colombo,[b] Claudia Conti,[b] Lara Gigli,[c] Marco Merlini,[a] Jasper Rikkert Plaisier,[c] Marco Realini,[b] G. Diego Gatta[a]

[a]*Dipartimento di Scienze della Terra, Università degli Studi di Milano, Via Botticelli 23, 20133 Milan, Italy*

[b]*Istituto per la Conservazione e la Valorizzazione dei Beni Culturali (ICVBC), Consiglio Nazionale delle Ricerche (CNR), Via R. Cozzi 53, 20125 Milan, Italy*

[c]*Elettra - Sincrotrone Trieste S.c.P.A., strada statale 14, 34149 Basovizza, Trieste, Italy*

**** Corresponding author: possenti@icvbc.cnr.it, Phone number: +39 02 66173386***

E-mail addresses: possenti@icvbc.cnr.it (E. Possenti, ORCID 0000-0002-9041-7971), c.colombo@icvbc.cnr.it (C. Colombo, ORCID 0000-0003-2735-539X), c.conti@icvbc.cnr.it (C. Conti, ORCID 0000-0002-5379-7995), lara.gigli@elettra.eu (L. Gigli), marco.merlini@unimi.it (M. Merlini, ORCID 0000-0002-1146-2468), jasper.plaisier@elettra.eu (J. R. Plaisier, ORCID 0000-0003-1981-1498), m.realini@icvbc.cnr.it (M. Realini, ORCID 0000-0002-7212-3806), diego.gatta@unimi.it (G. D. Gatta, ORCID 0000-0001-8348-7181)

Abstract

Many works of art are complex systems consisting of a core finished by the overlapping of several painted layers. In this work, we apply an innovative method based on grazing incidence X-ray diffraction (GIXRD) with synchrotron radiation (SR) to investigate polychrome stratigraphies with a completely non-destructive approach. The SR-GIXRD measurements provided direct and unambiguous compositional and stratigraphic information of the crystalline species lying in different layers. The investigations performed on a small fragment sampled from a painted terracotta statue allowed identifying pigments, fillers, aggregates of the matrix and newly formed decay salts in micrometric-thin paint layers. Furthermore, the great potentiality of this study is the feasibility of depth profile investigations on multi-layered painted samples from Cultural Heritage objects without resorting to cross sectional analyses. Currently, the method is non-destructive but it can be potentially non-invasive in situations where small moveable artworks can be placed into the measurement chamber of the SR-XRD beamlines. The overall study paves the way to a new scenario of artwork investigations, shading light on new unexplored approaches for non-destructive studies of Cultural Heritage objects, their conservation history and their interaction with the environment.

Introduction

The study of artistic artefacts is complex since on many of them an overlapping of several painted layers is present; moreover, every layer is usually composed by a mixture of different crystalline and amorphous phases dispersed in organic binders or inorganic fillers. The exhaustive and unambiguous characterization of the crystalline phase in the stratigraphy is crucial since each of them bring about new knowledge on the painting technique, the employed materials, their mutual interaction with aging, the presence of decay phases and/or products applied with conservation purposes.

One of the main goals of conservation science is to obtain the maximum amount of information with the minimum damage for the artwork. Furthermore, the samples available for analytical purposes are usually very small and unique; therefore, their preservation is crucial since they can be used for further investigations. In the last years, a very burning issue in the scientific community is the development of new analytical methods able to characterize artistic materials in a completely non-destructive modality.

Unfortunately, the conventional multi-analytical approach used to characterize pigments and crystalline phases in stratigraphic sequences requires the manipulation of the samples and it is usually destructive or micro-destructive: optical microscopy, conventional confocal Raman microscopy and scanning electron microscopy with energy dispersive X-ray spectroscopy (SEM-EDS) involve cross-sectional analyses (consisting on embedding the micro-fragments in organic resins to obtain polished cross sections or thin sections); X-ray powder diffraction (XRPD) or infrared spectroscopy (FT-IR) with KBr pellets require the grinding of the sample, whilst FT-IR with diamond cell or ATR need to compress it, etc. A significant step forward to the non-destructive study of pigments has been carried out.[1–6] In these studies the feasibility of a non-destructive depth profile study on layered artworks by micrometre-scale spatially offset Raman spectroscopy (micro-SORS) is demonstrated. However, this method is limited by the possible fluorescence emission of some compounds, the presence of weak Raman scatterers, the extremely heterogeneous layers, both in terms of composition and thickness.

A conventional diffractometric investigation might be the most suitable approach to characterize several pigments, but in many cases is not performable since XRPD requires a relative high amount of sample powder (highly destructive) and, even more important, it does not provide information about the stratigraphy. Micro-XRD,[7] synchrotron radiation (SR)-XRD and SR micro-XRD in transmission or reflection mode,[8–10] reduce the amount of sample necessary but, again, in many cases they requires the preparation of the sample.

On the other side, grazing incidence X-ray diffraction (GIXRD) is a powerful method for the surface investigation of thin films and of superimposed polycrystalline compounds,[11–15] providing information of metal alloys, corrosion products and potentially pigments.

The technique involves the investigation of the superficial portion of a material with small incidence angle (Φ) and collect the diffracted beam from a region below the surface.

The penetration depth (Δ) of X-rays inside a material depends on many variables, *e.g.* the X-ray wavelength, the composition of the materials (sample X-ray absorption) and the reflectance of X-rays.[16] The penetration depth is also influenced by the diffraction geometry and, in particular, by the incidence angle. GIXRD patterns can be collected from a crystalline material with a X-rays incidence angle equal or higher to the critical angle Φ_c, while below Φ_c, only the total external reflection due to refractive index occurs. Following that, as the incidence angle increases, the penetration depth of X-rays increases as well. As a consequence, by varying the Φ, it is possible to perform a depth profile study of crystalline phases collecting XRD pattern from different depth of the specimen.[17–19]

Despite the well-known potentiality of GIXRD to characterize thin films, only a few papers are available in literature on the use of GIXRD to study works of art. Most of them deal with the investigation of metallic artefacts,[19,20] historical mirrors,[17,18] alteration products on silicate glasses[21] and only a few with painted objects.[22–24]

Despite the possible application of GIXRD in cultural heritage diagnostic has been already suggested[7] and the feasibility of a depth profile study by varying the incidence angle (Φ) has been explored on historical mirrors and metals,[17–19,25] no data are available on the use of GIXRD for the depth profile study of pigments in a stratigraphy.

A GIXRD study is performable with laboratory instruments equipped with Göbel mirrors, as demonstrated by several authors.[19,21,25,26] However, in some cases, the use of SR might be necessary in order to study very thin layers composed of a mixture of crystalline phases and presenting compositional or thickness heterogeneity at the microscale.[18,23,27] In fact, SR facilities supply a highly energetic and monochromatic beam, a tunable wavelength or energy and a very small beam size, allowing the possible identification of trace phases in micrometric samples.

Hence, in this study we investigate the potentiality of GIXRD analysis to study the crystalline phases of pigments, fillers, aggregates of the matrix and decay products in real objects of Cultural Heritage and the feasibility of a depth profile study preserving the whole sample for further analytical insights. Furthermore, since painted layers are composed by several pigments, we demonstrate the GIXRD capability on identifying crystalline phases in complex mixture in a single measurement, overcoming the analytical limits of the punctual cross-sectional methods. The measurements were performed on mock-up specimens to optimize the acquisition set-up and on a fragment sampled from an historical terracotta statue (dates back to the end of the seventeenth century) of the UNESCO site Sacred Mounts of Ossuccio.

Materials and methods

Materials

Two different layered systems were *ad hoc* prepared to evaluate the potentiality of GIXRD. The first sample (S1) comprises a 3-layered system of commercial varnishes (pigments in acrylic binder) applied on a photographic paper. The second sample (S2) is a sequence of three thin disks (pigment in epoxy resin) artificially assembled over a sample holder. The sample S2, prepared in this way, allows maintaining a discontinuity between the thin disks in order to study the effects on GIXRD patterns of gaps between the painted layers. The pigments and the commercial varnishes

were previously characterized by powder XRD, FTIR and Raman spectroscopies. The layer sequence and the composition of each layer are reported in Table 1.

Mock-up stratigraphies						
Sample name	***Typology***	***Layer***	***Colour***	***Pigment composition***	***Fillers***	***Thickness***
S1	Overlapped commercial acrylic varnishes applied on photographic paper	1 (external)	Red	Hematite	Calcite, quartz, talc	60 µm
		2	White	Rutile, wollastonite, portlandite	Calcite, quartz, talc	60 µm
		3	Yellow	Clinobisvanite	Calcite, quartz, talc	500 µm
		Photographic paper	White		Kaolinite	-
S2	Thin sections in epoxy resin assembled over a sample holder	1 (external)	Violet	Ammonium cobalt phosphate hydrate		60 µm
		2	Yellow	Crocoite, phoenicrochroite	Gypsum, anhydrite, clinochlore	60 µm
		3	Red	Cinnabar		60 µm

Table 1 Scheme of the layer composition in mock-up stratigraphies

The sample S3 is from a painted statue of the UNESCO site Ossuccio Sacred Mount (Como, Italy). The site dates back in the range between the late 15th and 17th centuries and it consists in a series of devotional chapel containing wall paintings and polychrome sculptures. The small fragment was sampled from a terracotta sculpture conserved in VI chapel. The overlapping of several painted layers is due to the re-paintings carried out over the centuries with the aim to renew the hue of the surfaces for votive purposes. The morphology and composition of the stratigraphy was preliminary characterized with conventional destructive methods: sample embedded in polished cross section, SEM-EDS, FT-IR and Raman spectroscopy. A scheme of the layer succession of the fragment S3 is reported in Table 2.

Sample from real objects of Cultural Heritage					
Sample name	***Layer***	***Colour***	***Pigment composition***	***Other crystalline phases***	***Thickness***
S3	1 (external)	Dark yellow	Sodalite, goethite	Gypsum, weddellite, cotunnite, hydrocerussite, cerussite, calcite	100-120 µm
	2	Orange	Crocoite, phoenicrochroite, barite	Hydrocerussite, cerussite, calcite	20-80 µm
	3	Light red	Hematite, quartz, kaolinite		10-40 µm
	Bulk of the stucco	White		Calcite	-

Table 2 Scheme of the layer composition in the stratigraphy of real works of art

Methods

The X-ray diffraction measurements were performed in grazing incidence with synchrotron radiation (SR-GIXRD) at the MCX beamline[28] of the ELETTRA Italian Synchrotron facility (Trieste, Italy). The analyses were performed on the mock-up samples and on the artwork fragments without any sampling. The diffraction measurements were collected with the high-resolution four circle Huber diffractometer in the 2ϑ angular range of 1.5 – 50 °, step size of 0.01°, using a focalized monochromatic beam with λ = 0.82591(6) Å (exp. n°20167062). The Rietveld refinement on silicon standard was used to estimate the uncertainty of the experimental wavelength. The X-ray diffraction data were collected selecting a range of fixed incident grazing angles: Φ of 0.5, 1.0, 2.5 and 5.0 °, since small changes in Φ cause large variation in the penetration of X-rays through the material and this provides a depth profile on a larger micrometer scale. The minimal incidence angle of 0.5° has been chosen in order to collect a good diffraction pattern regardless of the surface roughness and to avoid the total reflection (*i.e.*, measurements above the critical angle).

The acquisition setup and the incidence angles were optimised considering the critical angle and the surface configuration in order to achieve a good signal/noise ratio. The X-ray beam spot size was 300 μm (vertical) x 500 μm (horizontal). A whole pattern profile fitting of the diffraction data was performed by the Rietveld method, using the GSAS package (http://www.ccp14.ac.uk/solution/gsas/; profile function: pseudo-Voigt, background function: Chebyshev polynomial). To fully understand the potentialities and limitations of the GIXRD approach, the pigmented layers of mock-up samples were firstly investigated as isolated layers. After that, they were assembled in a stratigraphic sequence and analysed with same setup used for the single layers.

Results and discussion

Fig. 1 shows the grazing incidence diffraction patterns over the increasing incidence angles of the mock-up sample S1. The crystalline phases used for the depth profile in mock-up samples, their marker interplanar distance and indexing, along with the relative PDF patterns used as references are shown in Table 3. In the GIXRD patterns, there are several well detectable crystalline phases. Calcite, talc and quartz peaks are present in all the GIXRD patterns and also in the GIXRD patterns of the references. These phases are added to the commercial formulates as fillers; therefore they were used as markers in the depth profile study of this sample.

The marker peaks of hematite in mixture with calcite are well evident in the GIXRD pattern collected at Φ of 0.5 ° and 1.0 °. In these two GIXRD patterns, the diffraction peaks of hematite are weak and quite broad, especially if compared to the calcite ones. This finding can be explained as follow: (i) in the varnish formulate, hematite is in low amounts with respect to calcite, as a very low fraction of iron oxide is able to give a deep red hue to the layer; (ii) the surface of the painted stratigraphy has a slight but intrinsic roughness which mainly affects the XRD reflection of crystalline phases in low amounts (as in this case, hematite), especially at very low incidence angles. No peaks of the underlying pigments are present in the GIXRD patterns at Φ of 0.5 ° and 1.0 °, indicating that with this two incidence angles only the most external pigmented layer has interacted with X-rays.

Moving from low to higher incidence angles, the intensity of the overall GIXRD pattern increases and the peaks of crystalline phases are sharper and better resolved. As previously observed,[29] this is due to the better X-ray scattering occurring at higher incidence angles and to the decrease of the noise effect of rough surfaces. The diffraction pattern collected at Φ of 2.5 ° shows the unambiguous increase of the XRD peaks of the white pigments of the second layer. In fact, in addition to hematite, the peaks of rutile and wollastonite are well resolved from the baseline. Despite portlandite is also present in the second layers (Table 1), no peaks of this phase are distinguishable, due to the severe overlapping with the peaks of other phases.

From the analysis of the peaks profile and the relative intensity of different peaks in the GIXRD at Φ of 5.0 °, it is possible to identify the presence of weak Bragg peaks of the last pigmented layers. In fact, the XRD peak at 2.92 Å and the shoulder at 3.09 - 3.08 Å demonstrate the interaction with the yellow layer composed of clinobisvanite. Moreover, the peak at 3.56 Å, visible both in the GIXRD pattern at 5.0 ° and in the white reference, is due to the basal (002) peak of kaolinite, ref. pattern 01-083-0971), the filler of the photographic paper, demonstrating the collection of the substrate diffraction signal as well.

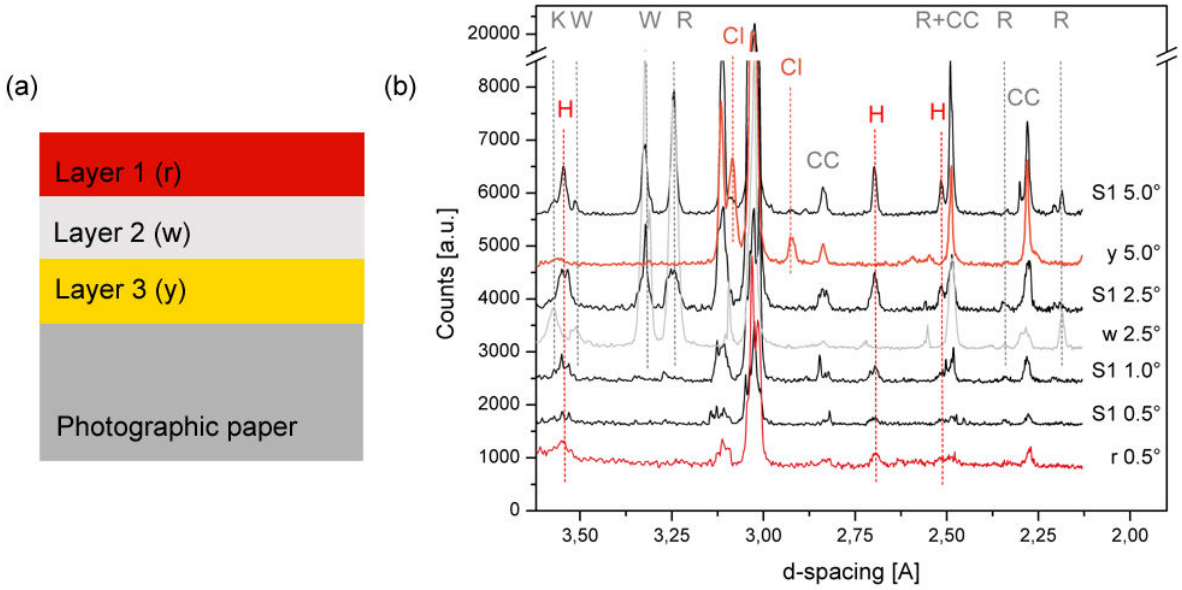

Fig.1 (a) Scheme of the layer succession and (b) GIXRD patterns of the mock-up sample S1 collected at different incidence angles (0.5 °, 1.0 °, 2.5 °, 5.0 °) in comparison with the reference patterns of red (r), yellow (y) and white (w) varnishes, collected at Φ of 0.5 °, 2.5 ° and 5.0 ° respectively. It is possible to observe the XRD peaks ascribable to hematite (H), rutile (R), wollastonite (W), clinobisvanite (Cl), calcite (CC) and kaolinite (K) of the photographic support

The sample S2 is another example of mock-up pigmented stratigraphy. In this case, the stratigraphic sequence was composed *in situ*, applying three separated pigmented thin disks on the sample holder. A slight gap remained between the thin sections, and the aim of the investigation was to evaluate how a discontinuity might affect the analyses, in terms of background noise and shift of the peak position. The GIXRD sequence collected on the sample S2 are shown in Fig. 2. The GIXRD patterns collected at 0.5 ° and 1.0 ° Φ strongly enhance the intensity of cobalt violet, the pigment of the most external disk. Also in this case, the diffraction peaks of the pigment located at 4.39 Å, 4.21

Å, 3.65 Å, 3.37 Å and 3.23 Å are weak and not well resolved. The same features occur in the reference, showing that this pattern is a characteristic mark of the low incidence XRD acquisitions.

When the investigations are performed at higher incidence angles, the peaks of the underlying disk rise from the baseline. In particular, in addition to cobalt violet, the XRD peaks of gypsum, crocoite, phoenicrochroite and anhydrite, are distinguishable in the diffractogram. The set of pigments detected by GIXRD is enriched of a further phase when the investigation moves to Φ of 5.0 °. In fact, in this last pattern, the growth of a shoulder at 3.35 Å and of a very weak peak at 3.16 Å shows the presence of cinnabar signal, arising from the disk lying at the bottom of the stratigraphic sequence. No particular shifts of interplanar distances are present for the yellow and red pigments, suggesting that the presence of a gap does not seem to interfere. It is worth noting that several pigments can be considered randomly oriented and weakly textured, as confirmed by their powder-like diffraction patterns. However, some pigments or some fillers, such as phyllosilicates, could have preferential orientations, with the occurrence of one or two very strong oriented diffraction peaks. Very strong, out-of-scale peaks are also expected by grinded pigments with preferential flaking planes, *e.g.* calcite, in which some GIXRD reflexes might be stronger than those in references or calculated patterns. An example is shown in Fig. 2, spectrum 2.5°, in which crocoite shows an extremely sharp and intense peak at about 3.47 Å.

Furthermore, GIXRD patterns are collected with a different geometry compared with the Bragg conditions and the investigated volume is different from an incidence angle to another. Following that, and considering the possible presence of strong peaks generated by preferential orientations, it is important to highlight that GIXRD measurements provide qualitative information but not quantitative or semi-quantitative data.

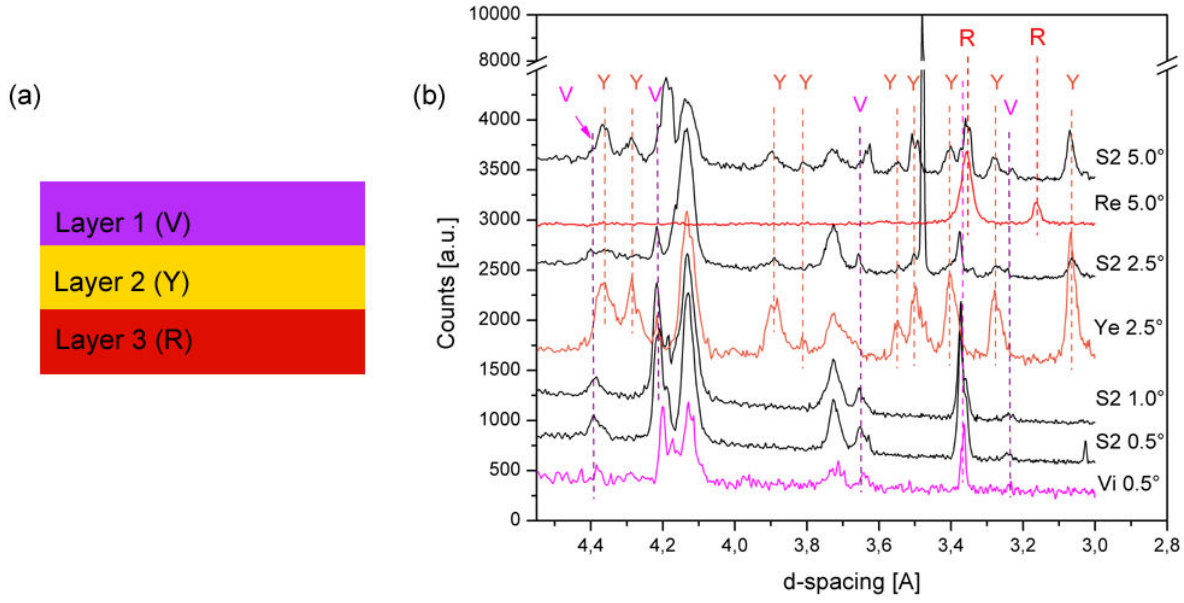

Fig.2 (a) Scheme of the layer succession and (b) GIXRD patterns collected at different incidence angles on the mock-up sample S2 at different Φ (0.5 °, 1.0°, 2.5°, 5.0 °) and GIXRD of reference patterns of the violet (Vi), yellow (Ye) and red (Re) disks collected at Φ of 0.5 °, 2.5 ° and 5.0 ° respectively. The XRD peaks of cobalt violet (V), pigments of the yellow layer (Y) and cinnabar (R) are observed

Mock-up stratigraphies			
Crystalline phase	***Chemical formula***	***Interplanar distances and indexing of the principal Bragg peaks***	***Reference pattern PDF***
Hematite	Fe_2O_3	3.67 Å (012), 2.69 Å (104), 2.51 Å (110)	01-089-0599
Calcite	$CaCO_3$	3.03 Å (104), 2.85 Å (006), 2.48 Å (110), 2.28 Å (113), 2.09 Å (202)	01-086-0174
Rutile	TiO_2	3.24 Å (110), 2.48 Å (101), 2.29 Å (200), 2.18 Å (111), 2.05 (210)	01-076-0679
Wollastonite	$CaSiO_3$	3.51 Å (002), 3.32 Å (-102), 2.97 Å (-220)	01-076-0186
Clinobisvanite or bismuth vanadate	$BiVO_4$	2.92 Å (040), 3.09 (-121), 3.08 Å (121)	00-014-0688
Kaolinite	$Al_2(Si_2O_5)(OH)_4$	3.56 Å (002)	01-083-0971
Cobalt violet	$NH_4CoPO_4 \cdot H_2O$	4.39 Å (002), 4.21 Å (011), 3.65 Å (110), 3.37 Å (111), 3.23 Å (012)	00-021-0793
Gypsum	$CaSO_4 \cdot 2H_2O$	4.27 Å (-121), 3.79 Å (040), 3.55 Å (130), 3.16 Å (-112)	01-074-1904
Crocoite	$PbCrO_4$	4.37 Å (-111), 3.27 Å (120)	01-073-2059
Phoenicrochroite	$PbO \cdot PbCrO_4$ or $Pb_2CrO_4(OH)_2$	3.39 Å (-310)	00-028-0530 or 00-008-0437
Anhydrite	$CaSO_4$	3.89 Å (111), 3.49 Å (020)	01-072-0503
Cinnabar (also known as vermillion)	HgS	3.35 Å (010), 3.16 Å (003)	00-042-1408

Table 3 Crystalline phases detected in the multi-layer profile of mock-up samples, their principal interplanar distances and indexing, and reference PDF patterns

The GIXRD analytical capability when dealing with real historic stratigraphies was carried out on the sample S3, a small fragment from the yellow garment of the stucco sculpture "sleeping man". The sample consists of over-painted layers with dark yellow pigments. The conventional cross-sectional analyses revealed the presence of three main layers, each one composed of a complex crystalline phases mixture of pigments and degradation by-products.

The most external layer (inhomogeneous thickness 100-120 μm) is dark yellow, and it is composed of low fraction of goethite with dispersed particles of sodalite, a blue silicate that origins the dark hue of the mantle. In the layer, there is also a mixture of decay products as gypsum, weddellite and lead chlorides (cotunnite). The underlying layer, with a warm orange tone (irregular thickness from 20 to 80 μm) contains a mixture of fine grained chrome-based yellow pigments (crocoite, lead (II) chromate, and phoenicrochroite) with barite particles. Between the first and the second layer there is a discontinuity, filled with organic matter. The most inner layer, characterized by a light red hue (thickness 10-40 μm), is made of red earth pigment (hematite with silicates). Some lead-based white compounds (hydrocerussite and cerussite) mixed with calcite are ever-present along the stratigraphy, therefore they were not used to study the depth profile of the pigments.

The GIXRD measurements collected on the sample S3 are plotted in Fig. 3. The main differences among the patterns at different angles can be deduced observing the spectra collected between 0.5-2.5 ° and 5° of Φ. At 0.5 ° and 1.0 ° of Φ the most external layer is mainly detected, showing the marker peaks of the decay by-products as gypsum at 7.57 Å and at 4.27 Å, and weddellite at 6.17 Å

and at 4.40 Å (Table 4). In the diffraction patterns for very small Φ, the low angle peaks are slightly shifted at lower 2 theta angles due to geometric effects. The sharp, well-defined, XRD peak of cotunnite is well resolved at 2.77 Å. Unfortunately, the other marker peaks of cotunnite are superimposed to the peaks of other phases. The GIXRD patterns at low incidence angles allow identifying also the blue pigment of the layer with a very good match with the PDF references. Weak peaks of sodalite, due to the low amount of the pigment in the layer, are also detected. However, goethite, the other pigment of the top layer, cannot be unambiguously identified in the GIXRD patterns, due to the severe superimposing of its marker peaks with gypsum and calcite ones. Two weak peaks at 5.44 Å and 4.41 Å in the GIXRD patterns collected at 0.5 ° and 1.0 ° of Φ are ascribable to crocoite, one of the pigments of layer 2 and its detection is most likely due to the presence of an irregularity in the thickness of the external layer.

The pigments of the layers 2 and 3 are well visible increasing the Φ. In fact, between 1.0 ° and 2.5 ° of Φ, the main Bragg peaks of crocoite, phoenicrochroite and barite are observable. The GIXRD patterns collected between 2.5° and 5.0 ° of Φ enhance the XRD weaker peaks of crocoite (at 2.54 Å, 2.05 Å and 2.04 Å) and reveal the pigments of the most inner layer: hematite with the peak at 2.51 Å, and kaolinite, with the peaks at 7.15 Å and 3.51 Å.

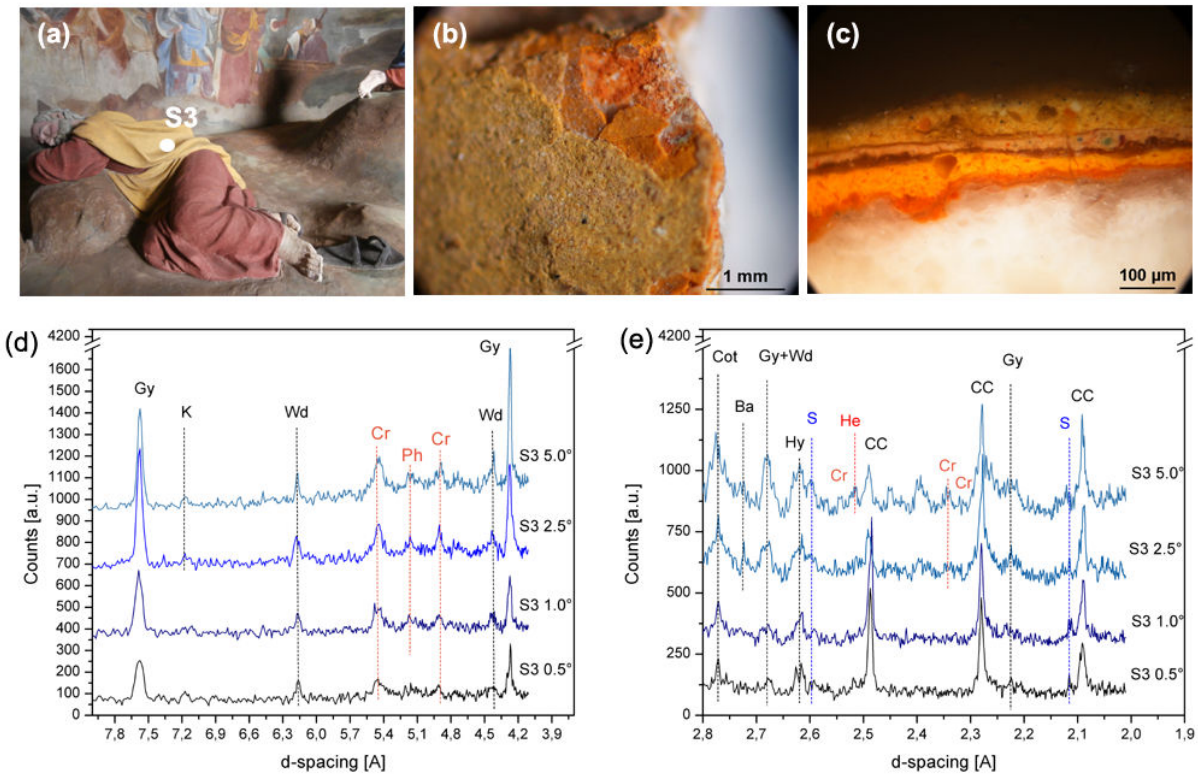

Fig.3 (a) Polychrome terracotta sculpture of the sleeping man and localization of the sampling area of fragment S3 (Ossuccio Sacred Mount); (b) fragment picture; (c) polished cross section; GIXRD patterns of the sample S3 collected at different Φ (0.5 °, 1.0°, 2.5°, 5.0 °) in the ranges 8-3.9 Å (d) and 2.8-1.9 Å (e). XRD reflexes of gypsum (Gy), kaolinite (K), weddellite (Wd), crocoite (Cr), phoenicrochroite (Ph), sodalite (S), barite (Ba), cotunnite (Cot), hematite (He), calcite (CC) and hydrocerussite (Hy)

Sample from real objects of Cultural Heritage

Crystalline phase	*Chemical formula*	*Interplanar distances and indexing of the principal Bragg peaks*	*Reference pattern PDF*
Gypsum	$CaSO_4 \cdot 2H_2O$	7.57 Å (020), 4.27 Å (-121)	00-006-0047
Weddellite	$Ca(CO_2)_2 \cdot (2+x)H_2O$	6.17 Å (200), 4.40 Å (121)	01-087-0655
Cotunnite	$PbCl_2$	2.77 Å (121)	00-001-0536
Sodalite	$Na_8(AlSiO_4)_6Cl_2$	4.02 Å (210), 3.67 Å (211), 3.18 Å (220), 2.59 Å (222), 2.11 Å (411), 2.01 Å (420)	01-088-2092 and 01-085-2067
Crocoite	PbCrO4	5.44 Å (-101), 4.41 Å (-111), 3.23 Å (021), 3.14 Å (210), 2.99 Å (-112), 2.54 Å (-212), 2.05 Å (301), 2.04 Å (-312)	01-073-1332
Phoenicrochroite	$PbO \cdot PbCrO_4$	5.17 Å (110)	01-076-0861
Barite	$BaSO_4$	3.43 Å (210), 3.09 Å (211), 2.72 Å (301)	01-076-0213
Hematite	Fe_2O_3	2.51 Å (110)	01-089-0599
Kaolinite	$Al_2(Si_2O_5)(OH)_4$	7.15 Å (002), 3.51 Å (112)	01-75-0938

Table 4 Crystalline phases detected in the multi-layer profile of real works of art, their marker interplanar distances and indexing, along with the reference PDF patterns

The findings demonstrate that the GIXRD method can be successfully used to obtain depth profiles of polychrome stratigraphies.

In fact, the GIXRD measurements coupled with SR are able to unambiguously identify at the microscale the crystalline phases of pigments, fillers, inorganic binders, aggregates and decay salts. The method provides information referred to a volume below the irradiated surface, averaging the possible compositional heterogeneity of the painted layers. This means that, notwithstanding using micrometric beam size, the technique can be considered a bulk analysis and not a punctual one, characterizing complex mixtures of pigment and trace phases with a reduced set of measurements. Following that, the GIXRD investigations allows decreasing the number of investigations of punctual cross-sectional techniques, focusing their analyses to specific, unsolved, issues (*e.g.* infrared spectroscopy to characterize organic compounds, cross sections to measure the thickness of the layers).

In spite of several advantages, the GIXRD technique has limitations as well. In fact, critical aspects are the composition of the crystalline phases, the surface topography and the layer succession.

Layers composed by a mixture of different minerals make difficult the identification, *e.g.* the same pigment can be present across different layers, precluding the possibility to use it as marker to distinguish the layers, or the markers peaks can have severe overlapping with other pigments. A further aspect is the texture of the substrate, which directly affects the collected diffraction pattern. In fact, the GIXRD technique requires a sample texture in which the compounds might be considered as finely grounded and randomly oriented. Big grains, phases organised with preferential orientation or poorly sorted grains are expected to produce XRD pattern not fully comparable to a "powder-like" one.

The surface topography and a regular layer succession are important parameters as well. In fact, the technique provides the best results investigating smooth surfaces and parallel layers, while very heterogeneous thickness and rough surfaces imply a more complex characterization. Extremely thin layers may not be discriminated by the adjacent ones and, in extreme situations, the GIXRD data

should be considered as average information on the tiny layer "surrounding". The GIXRD technique cannot provide information about the thickness of the layers.

Moreover, as already mentioned, GIXRD is a qualitative identification technique. An estimation of the relative quantity of a specific phase can be performed only comparing those phases that can be considered randomly oriented. Furthermore, from low to high Φ, the overall intensity of the patterns increases, due to the better X-ray scattering that occurs at higher incidence angle. Therefore, the increase of the intensity of XRD peaks from low to a high Φ should not be confused with the increase of the weight fraction of a given crystalline component.

Another aspect to consider is that some shift effects might origin from instrumental geometrical setup, making the XRD interpretation slightly more complex. In particular, the XRD peaks with high interplanar distances may undergo to a severe geometric shifts.

Conclusions

This study demonstrates the high potentiality of SR-GIXRD to study polychrome stratigraphic sequences with a fully non-destructive approach. By varying the incidence angle on the surface, the GIXRD method allows identifying the crystalline phases of painted layers, while SR allows investigating micrometric area obtaining a very good signal to noise ratio. The GIXRD technique can be used to identify the crystalline components in a very wide range of historical layered materials without any interference of the possible presence of organic fraction.

The SR-GIXRD provided qualitative phase information on the layer composition and on the conservation history of Cultural Heritage objects. At the same time, our study also focuses the attention on the possible limitations of the technique, namely: (i) no information on the thickness of the layers, (ii) the complexity to find markers of individual layers, especially in painted layers composed by a complex mixture of several pigments. The combination with other non-destructive techniques could be a winning solution to fully characterize unknown stratigraphies.

The method is applied to small fragments but it could be potentially applied to whole artistic mobile objects, developing an instrumental set-up able to contain bigger objects. This opens the scenario to a completely new characterization approach potentially able to characterize the surface and the inner portion of layered systems in general, *e.g.* study of fillers of historical papers, painted metals and painted objects in general, varnishes of archaeological pottery, decay products, inorganic-mineral conservative treatments.

Considering the potentialities of the method, the access to synchrotron radiation large scale facilities through periodic calls and the feasibility of a GIXRD study in almost all the SR-XRD beamlines, it is expected that SR-GIXRD will receive an increasing attention from the scientific community dealing with the depth profile investigations of Cultural Heritage materials and material science.

Conflict of Interest

There are no conflicts to declare

Acknowledgement

The authors gratefully acknowledge Dr Fabio Bevilacqua for the opportunity to study the Ossuccio Sacred Mount statuary and the Elettra - Synchrotron Trieste *S.c.P.A.* for the allocation of experimental beamtime through scientific proposal.

References

1 C. Conti, C. Colombo, M. Realini and P. Matousek, *J. Raman Spectrosc.*, 2015, **46**, 476–482.

2 C. Conti, C. Colombo, M. Realini, G. Zerbi and P. Matousek, *Appl. Spectrosc.*, 2014, **68**, 686–91.

3 C. Conti, M. Realini, C. Colombo and P. Matousek, *Analyst*, 2015, **140**, 8127–8133.

4 C. Conti, M. Realini, C. Colombo, A. Botteon and P. Matousek, *J. Raman Spectrosc.*, 2016, **47**, 565–570.

5 C. Conti, M. Realini, C. Colombo, A. Botteon, M. Bertasa, J. Striova, M. Barucci and P. Matousek, *Philos. Trans. R. Soc. A Math. Phys. Eng. Sci.*, 2016, **374**, 20160049.

6 M. Realini, C. Conti, A. Botteon, C. Colombo and P. Matousek, *Analyst*, 2017, **142**, 351–355.

7 C. Cardell, *Acta Crystallogr. Sect. A Found. Crystallogr.*, 2011, **67**, C109–C110.

8 E. Pouyet, B. Fayard, M. Salomé, Y. Taniguchi, F. Sette and M. Cotte, *Herit. Sci.*, 2015, **3**, 1–16.

9 E. Welcomme, P. Walter, P. Bleuet, J.-L. Hodeau, E. Dooryhee, P. Martinetto and M. Menu, *Appl. Phys. A*, 2007, **89**, 825–832.

10 J. Romero-Pastor, A. Duran, A. B. Rodríguez-Navarro, R. Van Grieken and C. Cardell, *Anal. Chem.*, 2011, **83**, 8420–8428.

11 G. Lim, W. Parrish, C. Ortiz, U. Brescia and M. Hart, *Mater. Res. Soc.*, 1987, **2**, 471–477.

12 P. Dutta, *Curr. Sci.*, 2000, **78**, 1478–1481.

13 S. J. Skrzypek, A. Baczmański, W. Ratuszek and E. Kusior, *J. Appl. Crystallogr.*, 2001, **34**, 427–435.

14 J. Rubio-Zuazo and G. R. Castro, *Rev. Adv. Mater. Sci.*, 2007, **15**, 79–86.

15 D. Simeone, C. Dodane-Thiriet, D. Gosset, P. Daniel and M. Beauvy, *J. Nucl. Mater.*, 2002, **300**, 151–160.

16 J. Als-Nielsen and D. McMorrow, *Elements of Modern X-ray Physics*, John Wiley & Sons, Inc., Hoboken, NJ, USA, 2011.

17 L. K. Herrera, A. Duran, M. L. Franquelo, M. del C. Jimenez de Haro, Á. Justo Erbez and J. L. Perez-Rodriguez, *J. Cult. Herit.*, 2008, **9**, e41–e46.

18 L. K. Herrera, A. Duran, M. L. Franquelo, A. R. González-Elipe, J. P. Espinós, J. Rubio-Zuazo, G. R. Castro, A. Justo and J. L. Perez-Rodriguez, *Cent. Eur. J. Chem.*, 2009, **7**, 47–53.

19 A. Duran, L. K. Herrera, M. del C. Jimenez de Haro, A. Justo and J. L. Perez-Rodriguez,

Talanta, 2008, **76**, 183–188.

20 L. K. Herrera, A. Justo, A. Muñoz-Páez, J. A. Sans and G. Martínez-Criado, *Anal. Bioanal. Chem.*, 2009, **395**, 1969–75.

21 T. Palomar, A. Chabas, D. M. Bastidas, D. de la Fuente and A. Verney-Carron, *J. Non. Cryst. Solids*, 2017, **471**, 328–337.

22 J. L. Perez-Rodriguez, M. del C. Jimenez de Haro, B. Siguenza and J. M. Martinez-Blanes, *Appl. Clay Sci.*, 2015, **116**–**117**, 211–219.

23 E. Dooryhée, M. Anne, I. Bardiès, J.-L. Hodeau, P. Martinetto, S. Rondot, J. Salomon, G. B. M. Vaughan and P. Walter, *Appl. Phys. A*, 2005, **81**, 663–667.

24 D. L. Floresta, M. Fagundes, J. D. Fabris and J. D. Ardisson, *Hyperfine Interact.*, 2015, **232**, 29–40.

25 D. Simeone, G. Baldinozzi, D. Gosset, S. Le Caer and J.-F. Bérar, *Thin Solid Films*, 2013, **530**, 9–13.

26 G. Chiari, A. Giordano and G. Menges, *Sci. Technol. Cult. Herit.*, 1996, **5**, 21–36.

27 L. K. Herrera and H. A. Videla, *Int. Biodeterior. Biodegradation*, 2009, **63**, 813–822.

28 J. R. Plaisier, L. Nodari, L. Gigli, E. Paz, R. San, R. Bertoncello and A. Lausi, *ACTA IMEKO*, 2017, **6**, 71–75.

29 E. Possenti, C. Colombo, C. Conti, L. Gigli, M. Merlini, J. R. Plaisier, M. Realini and G. D. Gatta, *Appl. Phys. A*, , DOI:10.1007/s00339-018-1798-8.